Spin polarized electron photoemission and detection studies

Ambar C. Rodríguez Alicea
Luca Cultrera, Brookhaven National Laboratory – Instrumentation Division
Oksana Chubenko, Arizona State University
Ratnakar Palai, University of Puerto Rico – Rio Piedras
Siddharth Karkare, Arizona State University

August 2022

Brookhaven National Laboratory
U.S. DEPARTMENT OF ENERGY

Polarized electron beam for accelerators

ILC, KEK

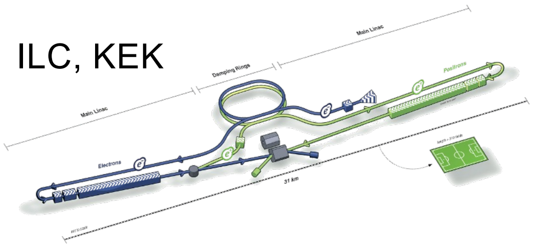

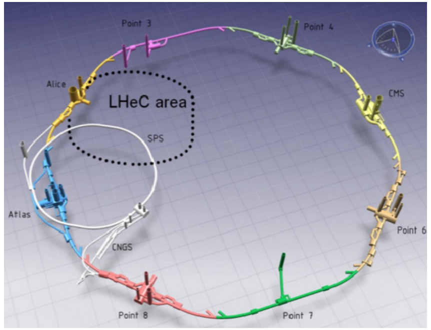

LHeC, CERN

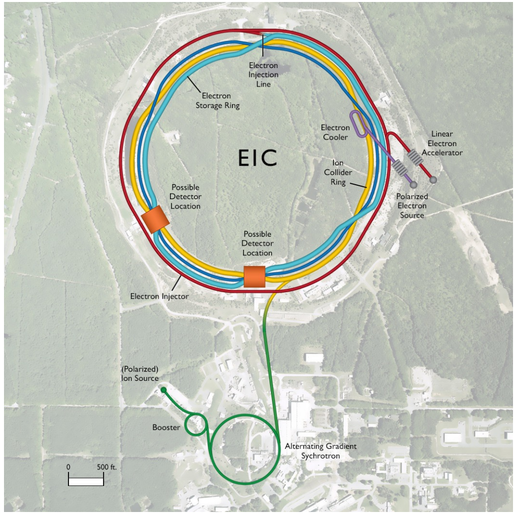

EIC, Brookhaven National Laboratory

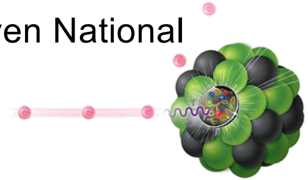

CEBAF, Jefferson National Laboratory

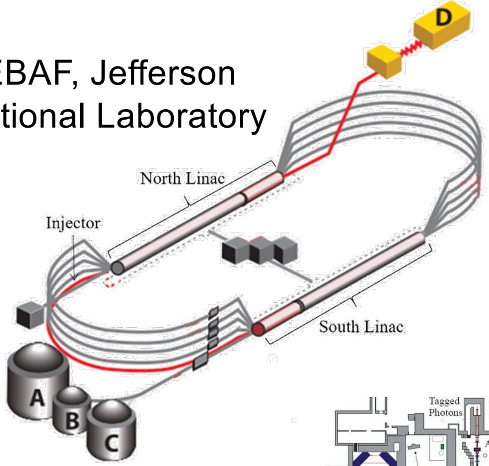

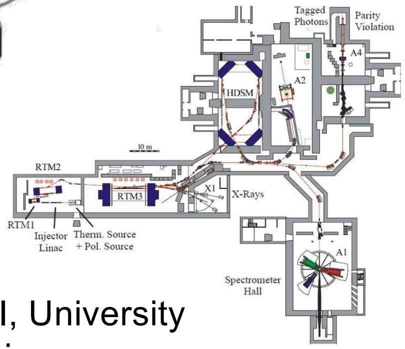

MAMI, University of Mainz

Production of polarized electrons

- There are three parameters that determine the performance of photocathodes

$$QE = \frac{\#\,electrons}{\#\,photons}\ ,\quad ESP = \frac{N^{\uparrow} - N^{\downarrow}}{N^{\uparrow} + N^{\downarrow}}\ \text{ and }\ 1/\tau = \ln\left(\frac{QE_o}{QE}\right)/t$$

- Advances in photocathode fabrication

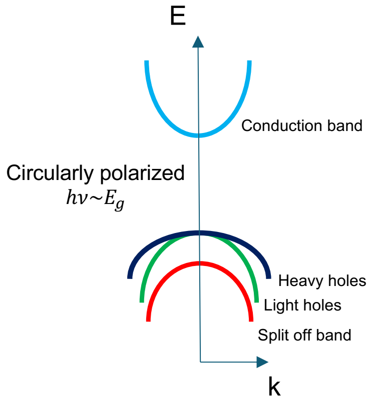

Bulk GaAs

QE ~ 10%
ESP ~ 40%

Polarization limited by energy degeneracy

1975

Production of polarized electrons

- There are three parameters that determine the performance of photocathodes

$$QE = \frac{\#\,electrons}{\#\,photons}\ ,\quad ESP = \frac{N^{\uparrow}-N^{\downarrow}}{N^{\uparrow}+N^{\downarrow}}\ \text{ and }\ 1/\tau = \ln\left(\frac{QE_o}{QE}\right)/t$$

- Advances in photocathode fabrication

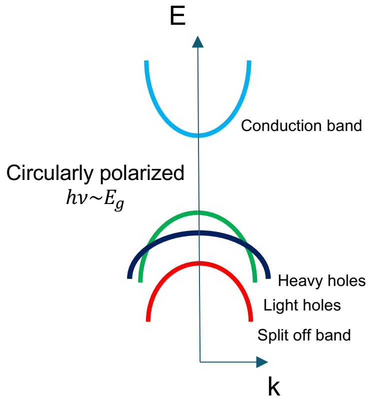

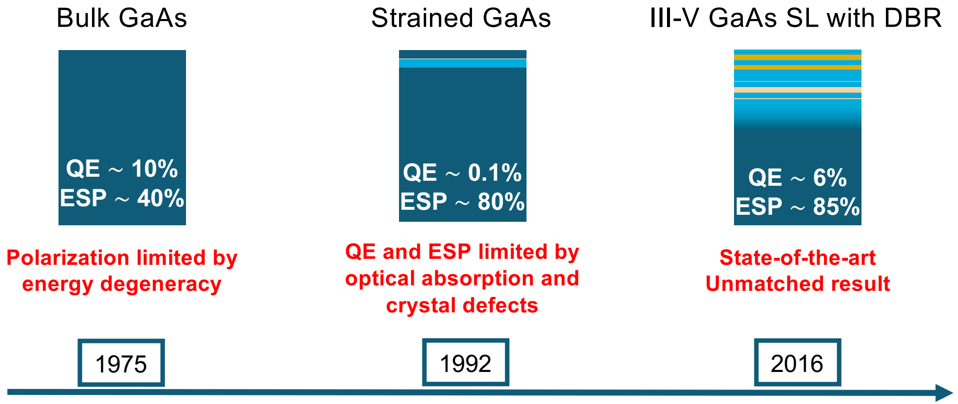

40 YEARS !!!

Negative electron affinity and lifetime

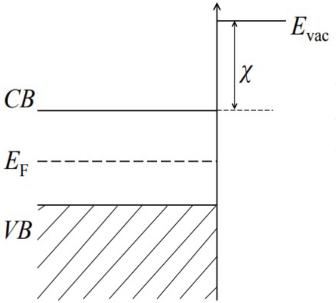

Cs-O or Cs-N-F_3 surface layers reduces χ_{eff}

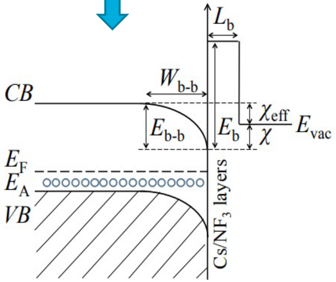

Chemical poisoning

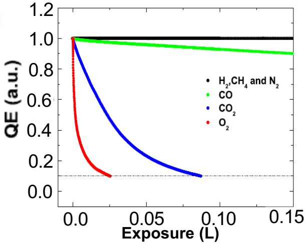

Alkali desorption

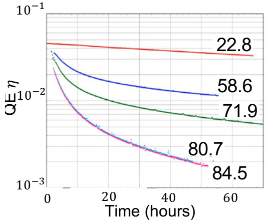

Ion back bombardment

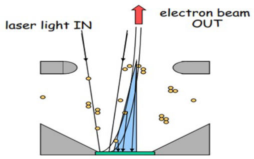

Challenges

- Extreme vacuum sensitivity
  - Deterioration of NEA layers

Brookhaven National Laboratory

Negative electron affinity and lifetime

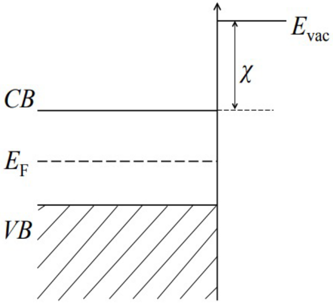

Cs-O or Cs-N-F_3 surface layers reduces χ_{eff}

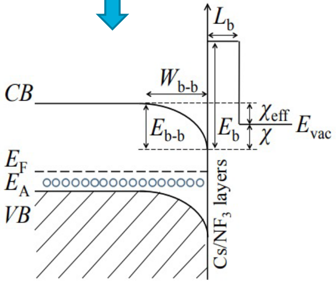

Chemical poisoning

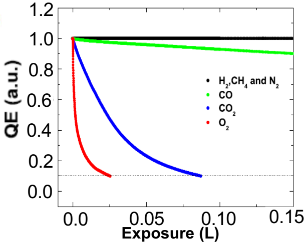

Alkali desorption

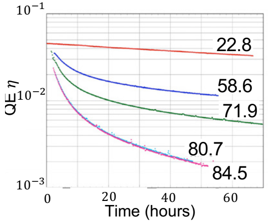

Ion back bombardment

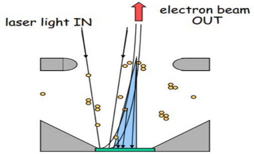

Challenges

- Extreme vacuum sensitivity
  - Deterioration of NEA layers
- Complex layered structure

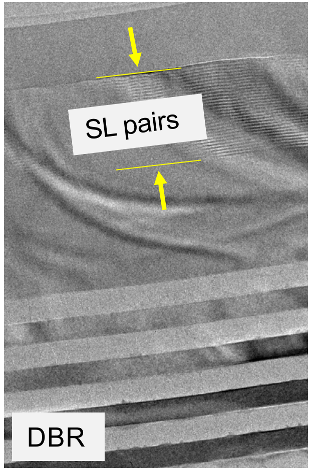

GaAs	5 nm	p = 5x10^{19} cm^{-3}
$GaAs_{0.62}P_{0.38}$	4 nm	p = 5x10^{17} cm^{-3}
GaAs	4 nm	p = 5x10^{17} cm^{-3}
$GaAs_{0.81}P_{0.19}$	300 nm	p = 5x10^{18} cm^{-3}
$AlAs_{0.78}P_{0.22}$	65 nm	p = 5x10^{18} cm^{-3}
$GaAs_{0.81}P_{0.19}$	55 nm	p = 5x10^{18} cm^{-3}
$GaAs_{0.81}P_{0.19}$	2000 nm	p = 5x10^{18} cm^{-3}
GaAs->$GaAs_{0.81}P_{0.19}$	2750 nm	p = 5x10^{18} cm^{-3}
GaAs buffer	200 nm	p = 5x10^{18} cm^{-3}
GaAs substrate		p > 1x10^{18} cm^{-3}

85 layers!!!

Brookhaven National Laboratory

Alternative to GaAs?

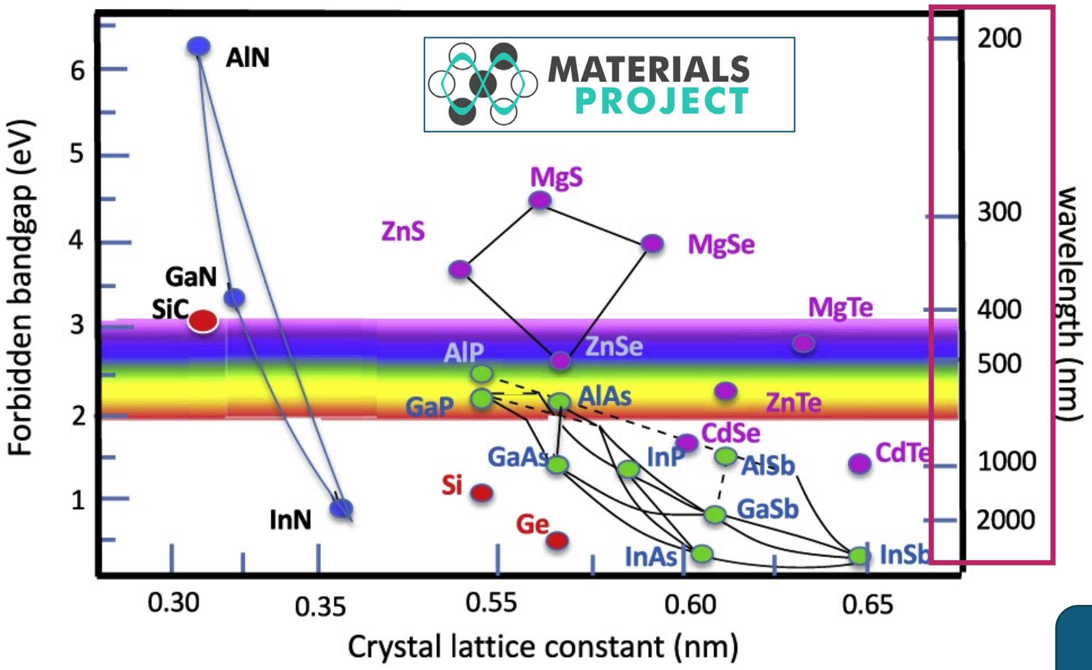

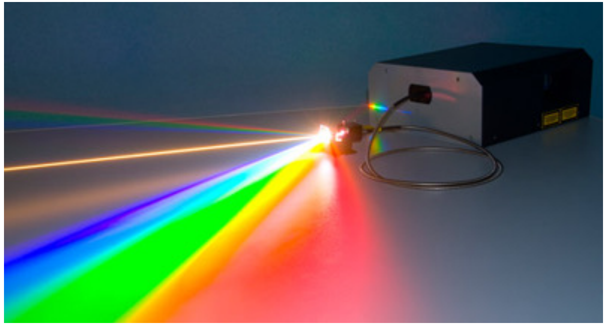

We want to screen new candidate materials quickly

Framework that combines DFT and Monte Carlo simulation of photoemission

Method: DFT + Monte Carlo

- Monte Carlo simulation of polarized electron emission from bulk GaAs reproduces experimental results

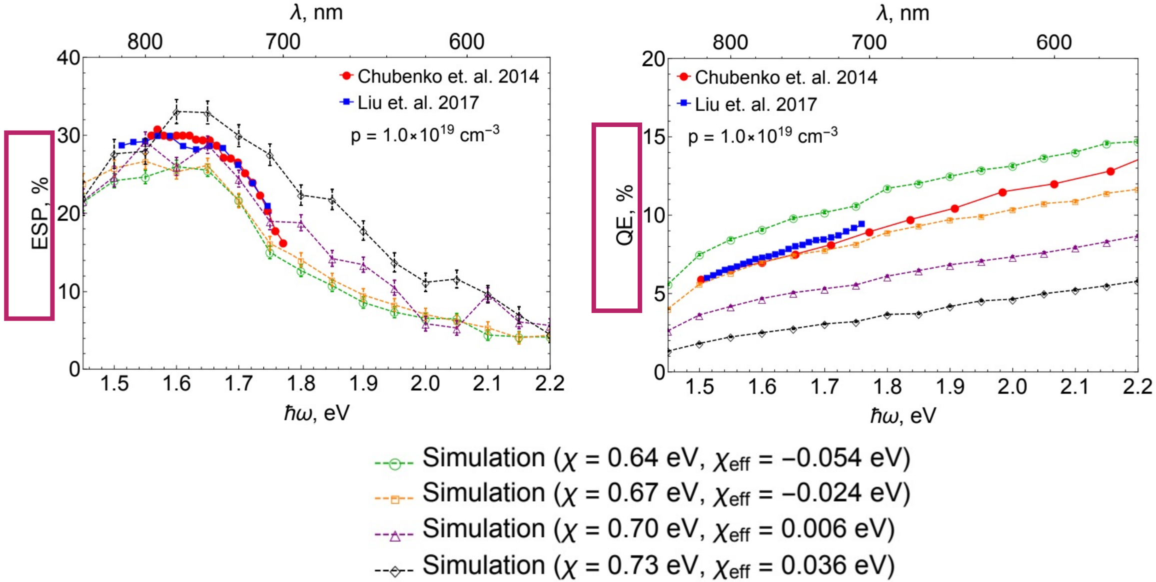

Symbol	Meaning, units	Value [Ref.]
Band model parameters		
m^*_Γ	Electron effective mass in Γ valley, m_0	0.063 [29]
m^*_L	Electron effective mass in L valley, m_0	0.22 [10]
m^*_X	Electron effective mass in X valley, m_0	0.58 [10]
α_Γ	Non-parabolicity factor for Γ valley, eV^{-1}	0.61 [10]
α_L	Non-parabolicity factor for L valley, eV^{-1}	0.461 [10]
α_X	Non-parabolicity factor for X valley, eV^{-1}	0.204 [10]
m^*_{hh}	hh effective mass, m_0	0.50 [29]
m^*_{lh}	lh effective mass, m_0	0.088 [29]
m^*_{so}	so effective mass, m_0	0.15 [30]
E_{g0}	Intrinsic band gap energy, eV	1.423 [29]
Δ_{so}	Split-off energy gap, eV	0.332 [30]
$\Delta_{\Gamma L}$	Energy splitting between minima of Γ and L valleys, eV	0.284 [29]
$\Delta_{\Gamma X}$	Energy splitting between minima of Γ and X valleys, eV	0.476 [29]
Momentum relaxation parameters		
$\Xi_{d\Gamma}$	Acoustic deformation potential for Γ valley, eV	7.01 [10]
Ξ_{dL}	Acoustic deformation potential for L valley, eV	9.2 [10]
Ξ_{dX}	Acoustic deformation potential for X valley, eV	9.0 [10]
$\hbar\omega_0$	Polar optical phonon energy, meV	35.36 [10]
$D_{\Gamma L}$	Deformation potential for $\Gamma \to L$ scattering, eV Å^{-1}	10 [10]
$D_{\Gamma X}$	Deformation potential for $\Gamma \to X$ scattering, eV Å^{-1}	10 [10]
D_{LL}	Deformation potential for $L \to L$ scattering, eV Å^{-1}	10 [10]
D_{LX}	Deformation potential for $L \to X$ scattering, eV Å^{-1}	5 [10]
D_{XX}	Deformation potential for $X \to X$ scattering, eV Å^{-1}	7 [10]
$\hbar\omega_{\Gamma L}$	Intervalley phonon energy for $\Gamma \to L$ scattering, meV	27.8 [10]
$\hbar\omega_{\Gamma X}$	Intervalley phonon energy for $\Gamma \to X$ scattering, meV	29.9 [10]
$\hbar\omega_{LL}$	Intervalley phonon energy for $L \to L$ scattering, meV	29 [10]
$\hbar\omega_{LX}$	Intervalley phonon energy for $L \to X$ scattering, meV	29.3 [10]
$\hbar\omega_{XX}$	Intervalley phonon energy for $X \to X$ scattering, meV	29.9 [10]
Z_Γ	Number of equivalent Γ valleys to scatter into	1 [31]
Z_L	Number of equivalent L valleys to scatter into	4 [31]
Z_X	Number of equivalent X valleys to scatter into	3 [31]
Spin relaxation parameters		
A_{ap}	EY constant for scattering by acoustic phonons	32/27 [21]
A_{pop}	EY constant for scattering by polar optical phonons	32/27 [21]
A_{ij}	EY constant for intervalley scatterings	32/27 [21]
A_{ii}	EY constant for scattering by ionized impurities	32/27 [21]
Q_{ap}	DP constant for scattering by acoustic phonons	1/6 [21]
Q_{pop}	DP constant for scattering by polar optical phonons	1/6 [21]
Q_{ij}	DP constant for intervalley scatterings	1/6 [21]
Q_{ii}	DP constant for scattering by ionized impurities	1/6 [21]
Δ_{exc}	Exchange splitting of exciton ground state, μeV	47 [22]
$\lvert\psi(0)\rvert^2$	Sommerfeld factor	1 [28]
Other material parameters		
ϵ_∞	High-frequency dielectric constant, ϵ_0	10.92 [10]
ϵ_s	Static dielectric constant, ϵ_0	12.90 [10]
ρ	Crystal density, kg m^{-3}	5360 [10]
v_s	Sound velocity, m s^{-1}	5240 [10]

Brookhaven National Laboratory

O. Chubenko, S. Karkare, D. A. Dimitrov, J. K. Bae, L. Cultrera, I. Bazarov, and A. Afanasev, Journal of Applied Physics, vol. 130, no. 6, p. 063101, 2021.

Method: DFT + Monte Carlo

QUANTUMESPRESSO

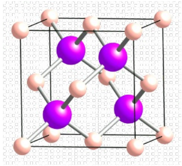

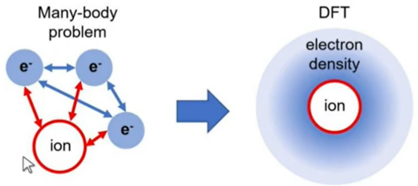

Electronic band structure

Phonon dispersion energies

Complex dielectric properties

Band model parameters		
m^*_Γ	Electron effective mass in Γ valley, m_0	0.063 [29]
m^*_L	Electron effective mass in L valley, m_0	0.22 [10]
m^*_X	Electron effective mass in X valley, m_0	0.58 [10]
α_Γ	Non-parabolicity factor for Γ valley, eV^{-1}	0.61 [10]
α_L	Non-parabolicity factor for L valley, eV^{-1}	0.461 [10]
α_X	Non-parabolicity factor for X valley, eV^{-1}	0.204 [10]
m^*_{hh}	hh effective mass, m_0	0.50 [29]
m^*_{lh}	lh effective mass, m_0	0.088 [29]
m^*_{so}	so effective mass, m_0	0.15 [30]
E_{g0}	Intrinsic band gap energy, eV	1.423 [29]
Δ_{so}	Split-off energy gap, eV	0.332 [30]
$\Delta_{\Gamma L}$	Energy splitting between minima of Γ and L valleys, eV	0.284 [29]
$\Delta_{\Gamma X}$	Energy splitting between minima of Γ and X valleys, eV	0.476 [29]
Momentum relaxation parameters		
$\Xi_{d\Gamma}$	Acoustic deformation potential for Γ valley, eV	7.01 [10]
Ξ_{dL}	Acoustic deformation potential for L valley, eV	9.2 [10]
Ξ_{dX}	Acoustic deformation potential for X valley, eV	9.0 [10]
$\hbar\omega_0$	Polar optical phonon energy, meV	35.36 [10
$D_{\Gamma L}$	Deformation potential for $\Gamma \to L$ scattering, eV Å^{-1}	10 [10]
$D_{\Gamma X}$	Deformation potential for $\Gamma \to X$ scattering, eV Å^{-1}	10 [10]
D_{LL}	Deformation potential for $L \to L$ scattering, eV Å^{-1}	10 [10]
D_{LX}	Deformation potential for $L \to X$ scattering, eV Å^{-1}	5 [10]
D_{XX}	Deformation potential for $X \to X$ scattering, eV Å^{-1}	7 [10]
$\hbar\omega_{\Gamma L}$	Intervalley phonon energy for $\Gamma \to L$ scattering, meV	27.8 [10]
$\hbar\omega_{\Gamma X}$	Intervalley phonon energy for $\Gamma \to X$ scattering, meV	29.9 [10]
$\hbar\omega_{LL}$	Intervalley phonon energy for $L \to L$ scattering, meV	29 [10]
$\hbar\omega_{LX}$	Intervalley phonon energy for $L \to X$ scattering, meV	29.3 [10]
$\hbar\omega_{XX}$	Intervalley phonon energy for $X \to X$ scattering, meV	29.9 [10]
Other material parameters		
ϵ_∞	High-frequency dielectric constant, ϵ_0	10.92 [10]
ϵ_s	Static dielectric constant, ϵ_0	12.90 [10]

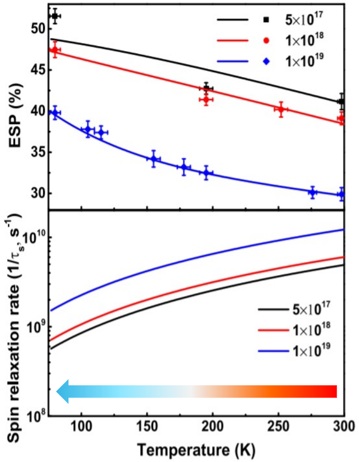

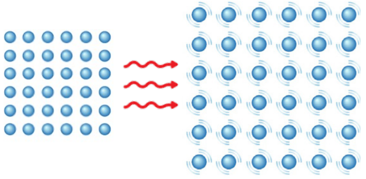

DFT calculations result

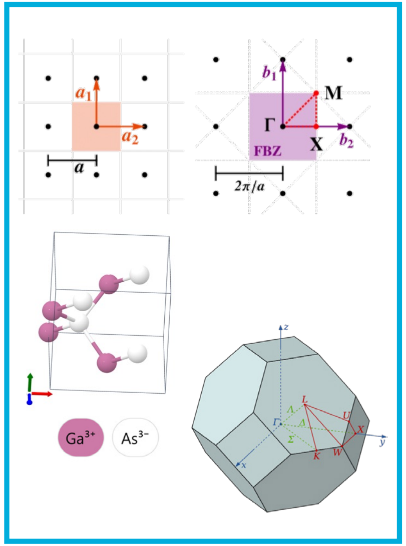

Electronic band structure

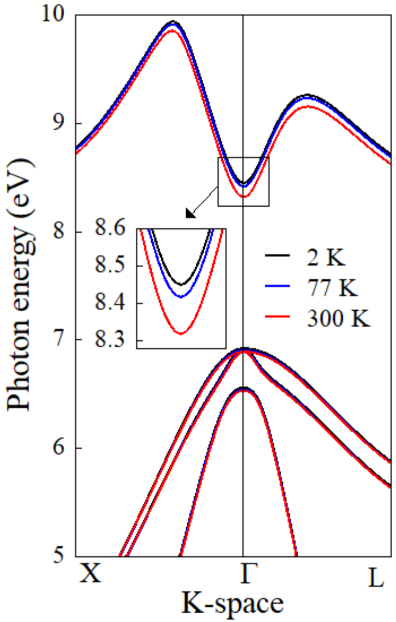

Phonon dispersion

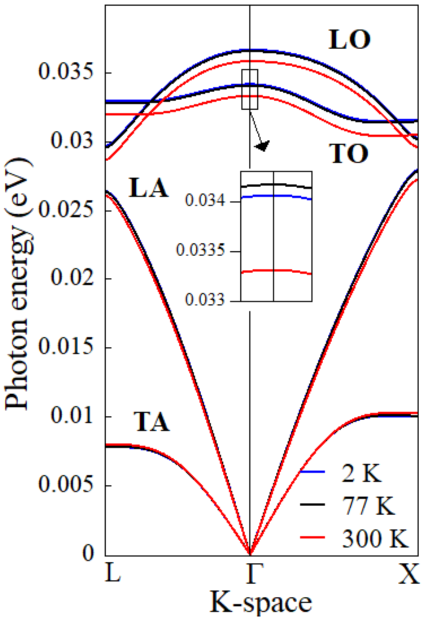

Absorption and reflectance

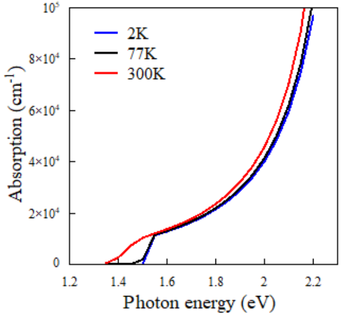

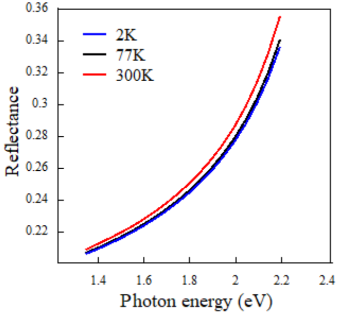

Result parameters

Parameter		Obtained 2 K	Obtained 77 K	Obtained 300 K	Reference 300 K
Electron effective mass (m*)	CB – X	0.295	0.282	0.283	0.58
	CB – G	0.069	0.068	0.066	0.063
	CB – L	0.13	0.13	0.129	0.22
	HH	0.368	0.368	0.374	0.50
	LH	0.08	0.08	0.079	0.088
	SO	0.118	0.117	0.114	0.15
Energy gap (eV)	Intrinsic	1.52	1.51	1.42	1.42
	Split-off	0.362	0.361	0.36	0.332
Splitting energy (eV)	G – L	0.008	0.024	0.034	0.284
	G – X	0.315	0.33	0.381	0.476
Non-parabolicity factor (eV^{-1})	G	0.571	0.574	0.611	0.61
	L	0.498	0.5	0.532	0.461
	X	0.328	0.341	0.36	0.204
Optical parameters	H.f. dielectric (ϵ_o)	11.40	11.43	11.49	10.92
	Static dielectric (ϵ_o)	11.79	11.82	11.90	12.90
Polar optical phonon energy, meV		35.0	34.9	34.1	35.36
Intervalley scattering phonon energy (meV)	Γ → L	31.8	31.7	29.7	27.8
	Γ → X	31.1	30.9	29.7	29.9
	L → L	31.8	31.7	29.7	29
	L → X	31.5	31.3	29.7	29.3
	X → X	31.8	31.7	29.7	29.9
Crystal density, kg m^{-3}		5640	5632	5605	5360
Sound velocity, m s^{-1}		5127	5125	5240	5004

Parameter		Value
Deformation potential for scattering (eV °A^{-1})	Γ → L	10
	Γ → X	10
	L → L	10
	L → X	5
	X → X	7
Acoustic deformation potential (eV)	L	9.2
	X	9.0
	Γ	7.01
Number of equivalent valleys to scatter	Γ	1
	L	4
	X	3
EY constants	scattering by acoustic phonons	32/27
	scattering by polar optical phonons	32/27
	intervalley scatterings	32/27
	scattering by ionized impurities	32/27
DP constants	scattering by acoustic phonons	1/6
	scattering by polar optical phonons	1/6
	intervalley scatterings	1/6
	scattering by ionized impurities	1/6
Exchange splitting of exciton ground state, μeV		47
Sommerfeld factor		1

Monte Carlo Simulation

Brookhaven National Laboratory

Simulation of photoemission

- One free parameter fits polarization and QE simultaneously
- Increased in polarization with lowering temperature

Effective electron affinity

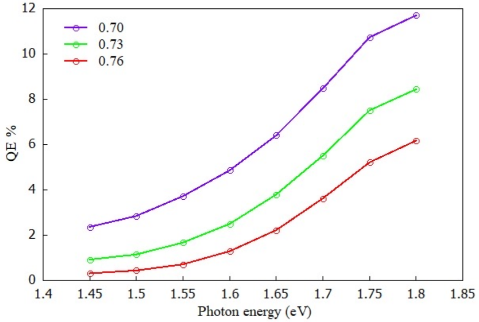

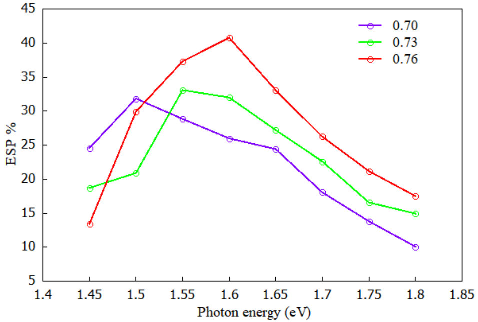

W. Liu, M. Poelker, X. Peng, S. Zhang, and M. Stutzman, Journal of Applied Physics, vol. 122, p. 035703, 07 2017

Simulation of photoemission

- One free parameter fits polarization and QE simultaneously
- Increased in polarization with lowering temperature

Predictions for new materials and structures

Effective electron affinity

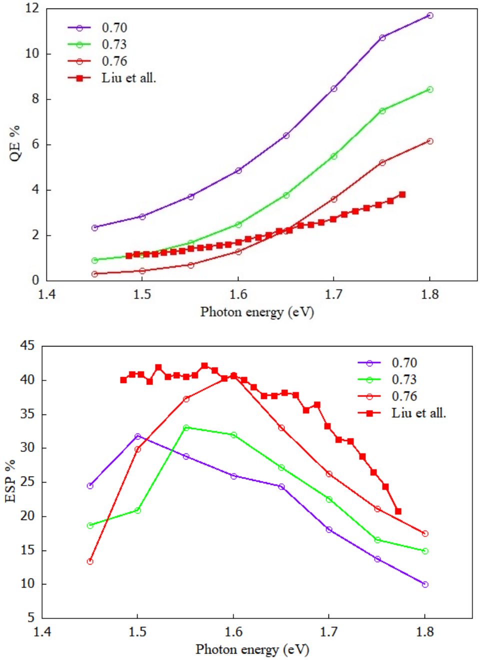

Temperature dependence

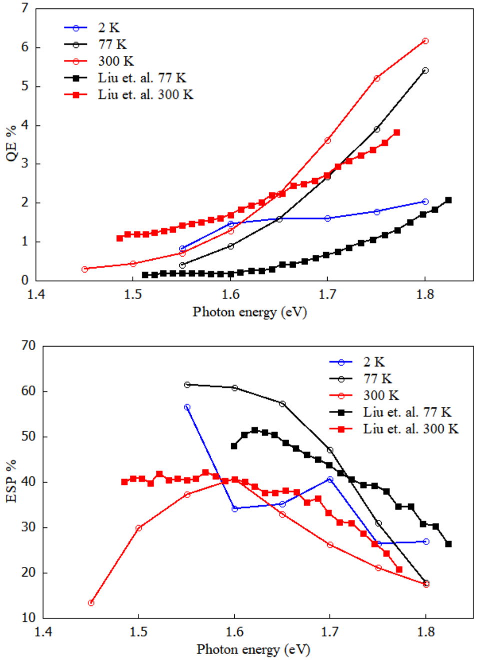

W. Liu, M. Poelker, X. Peng, S. Zhang, and M. Stutzman, Journal of Applied Physics, vol. 122, p. 035703, 07 2017

System for electron beam polarization detection

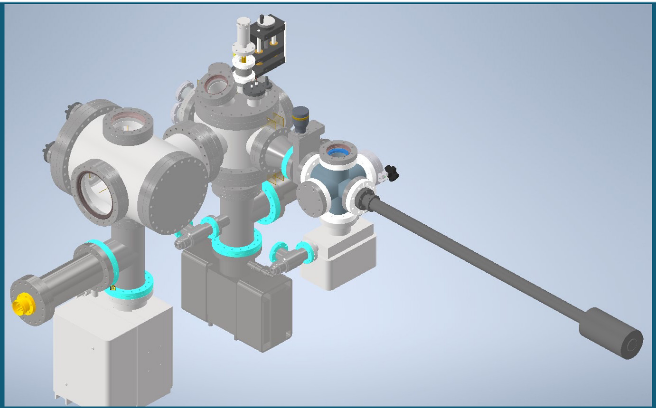

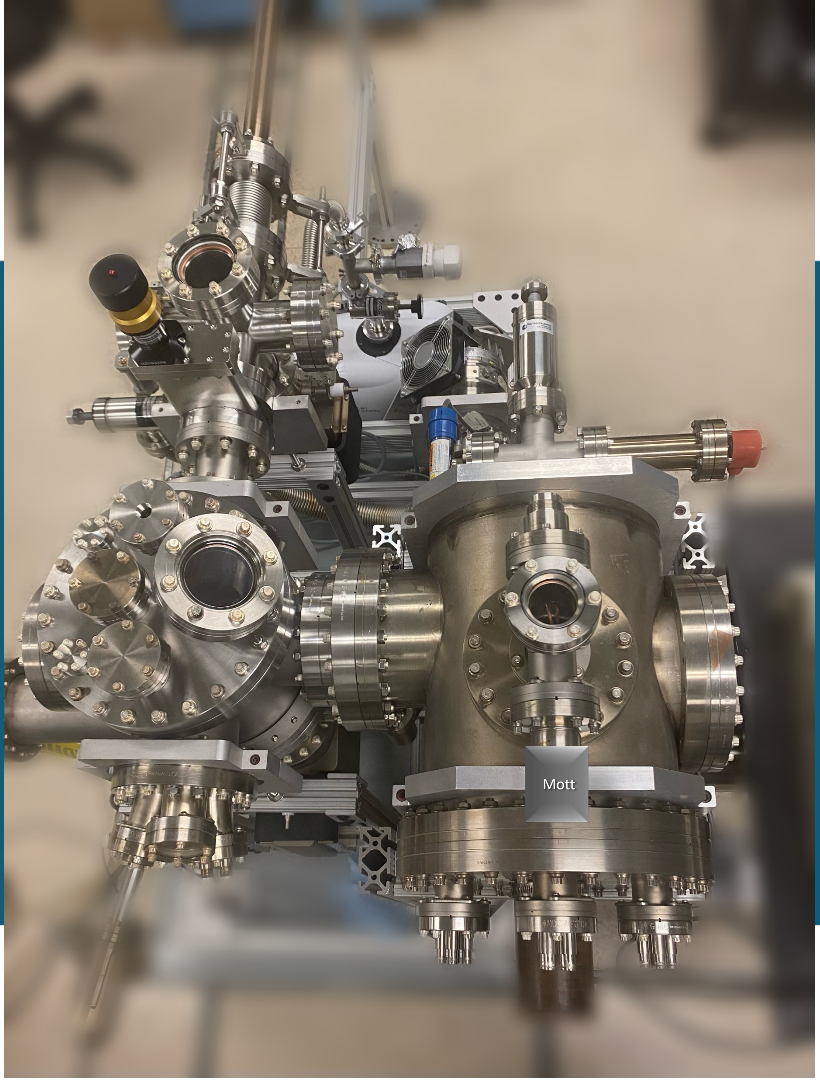

System for electron beam polarization detection

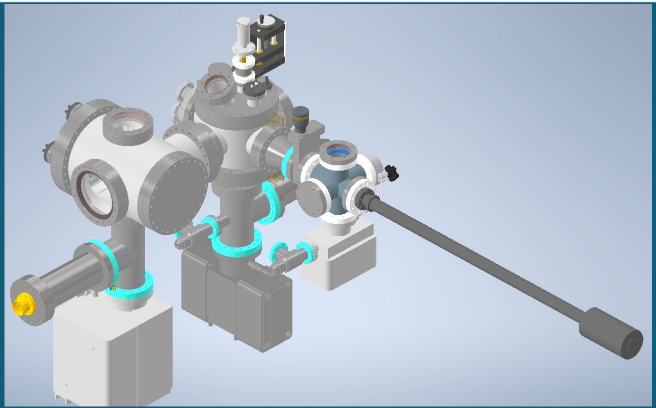

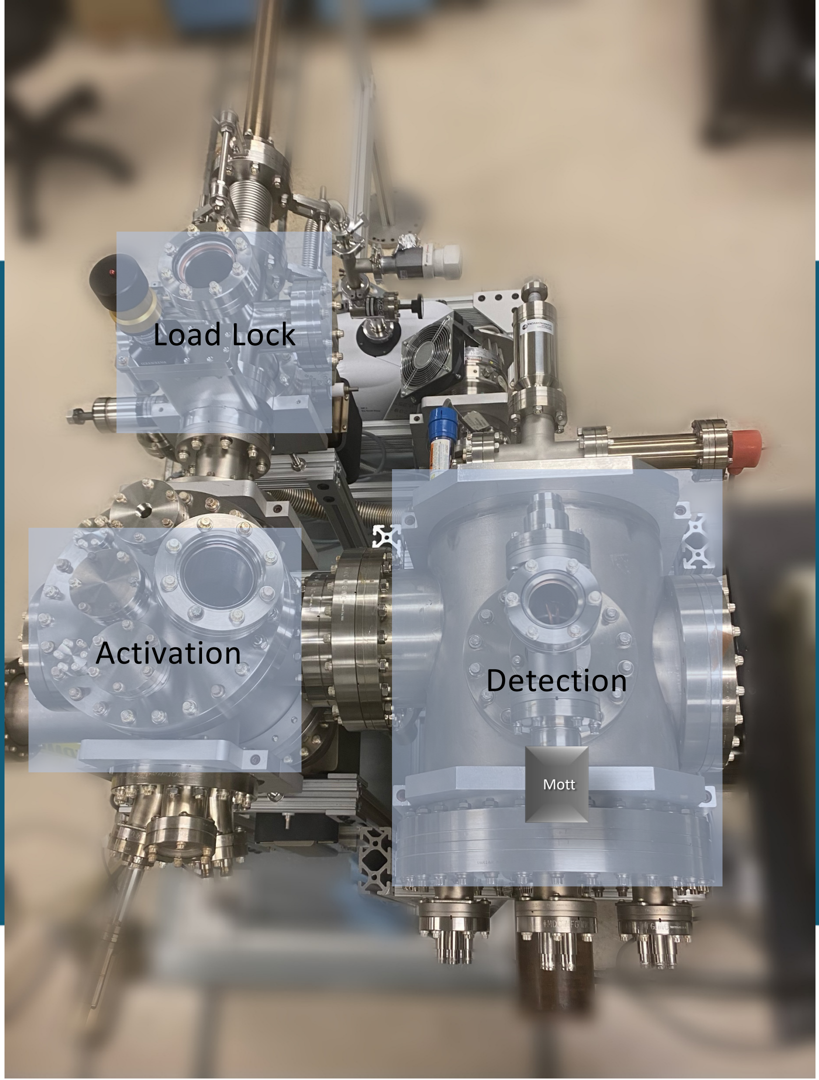

System for electron beam polarization detection

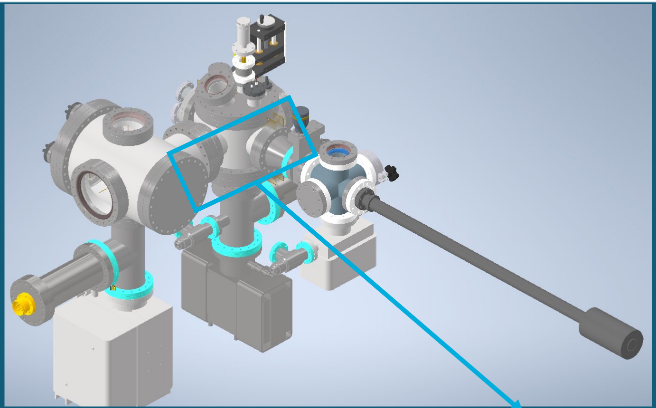

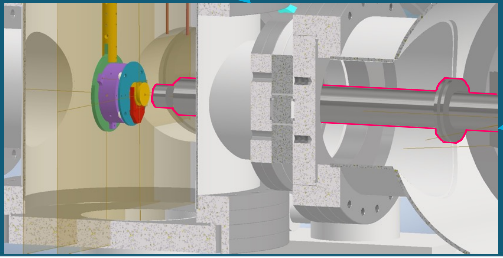

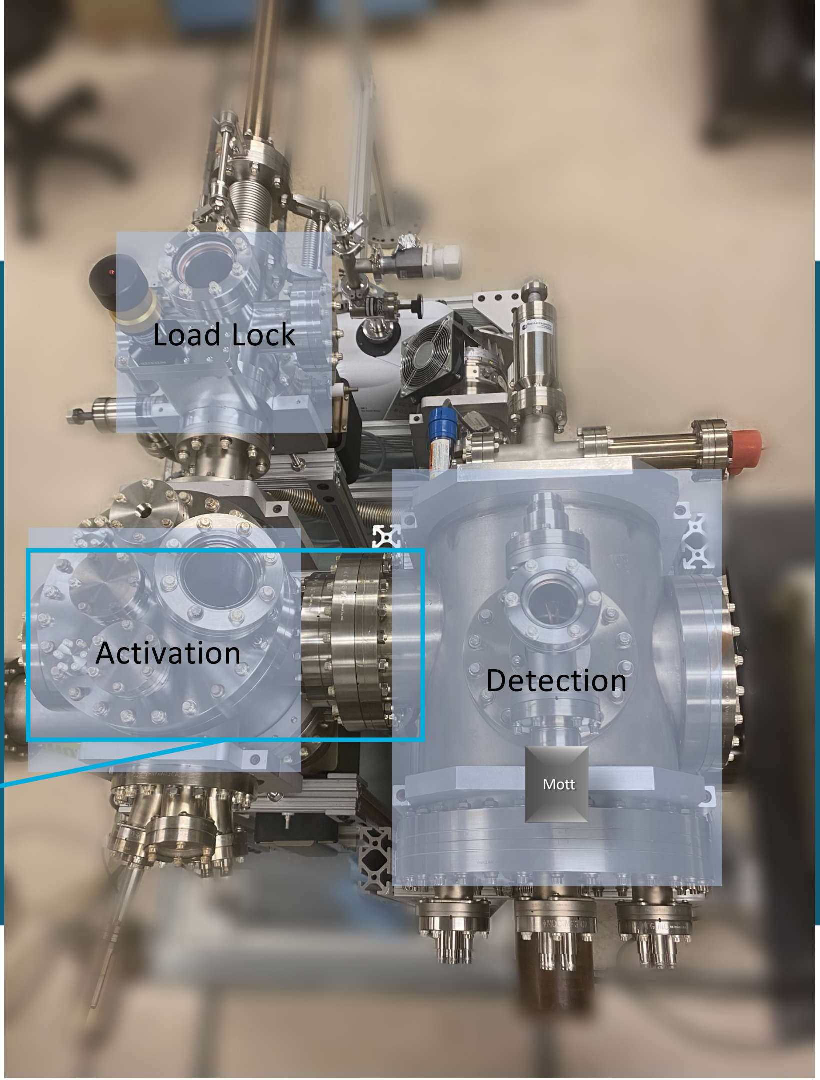

System for electron beam polarization detection

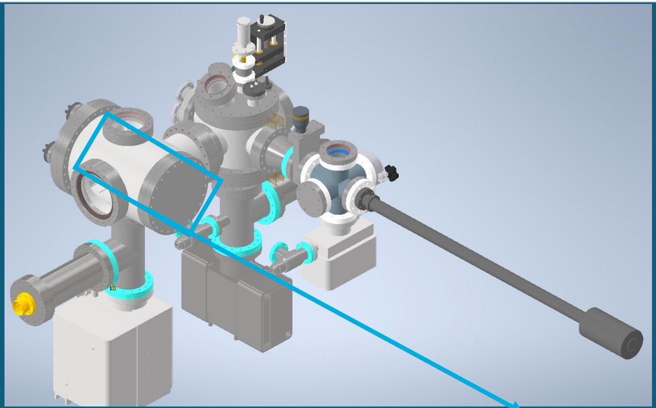

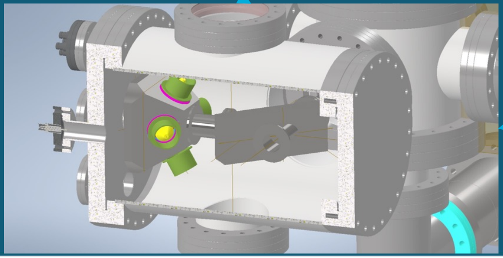

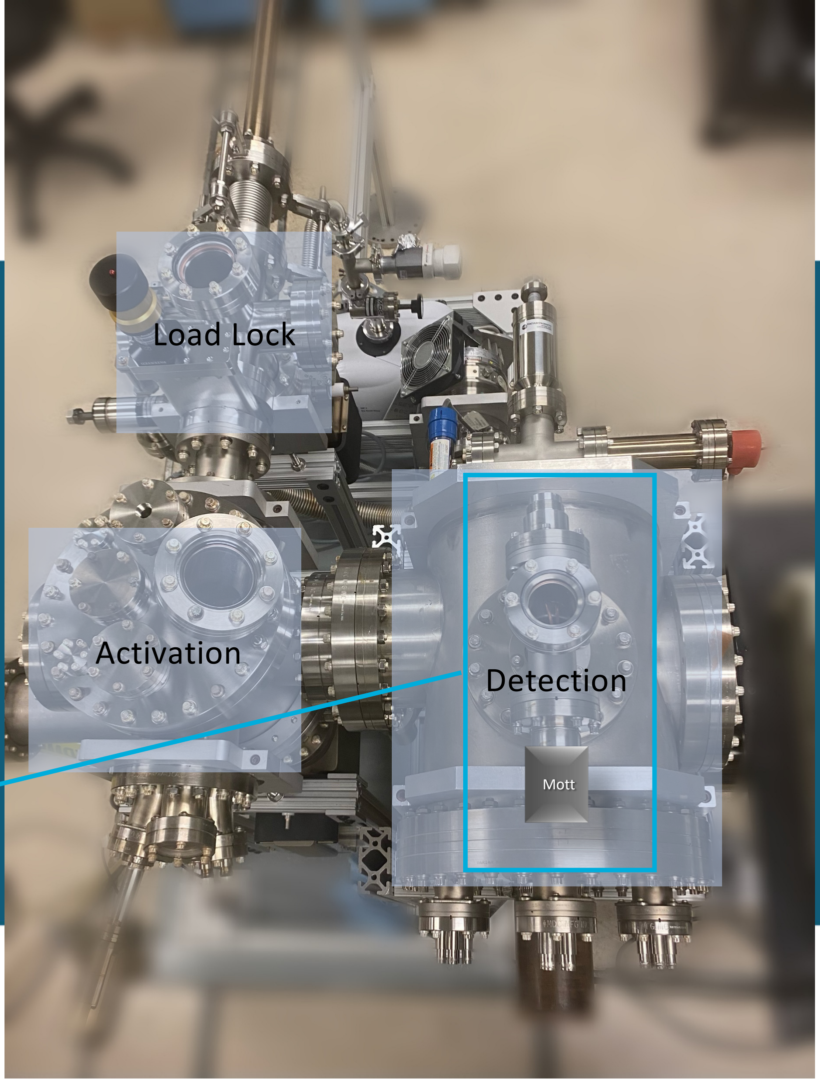

System for electron beam polarization detection

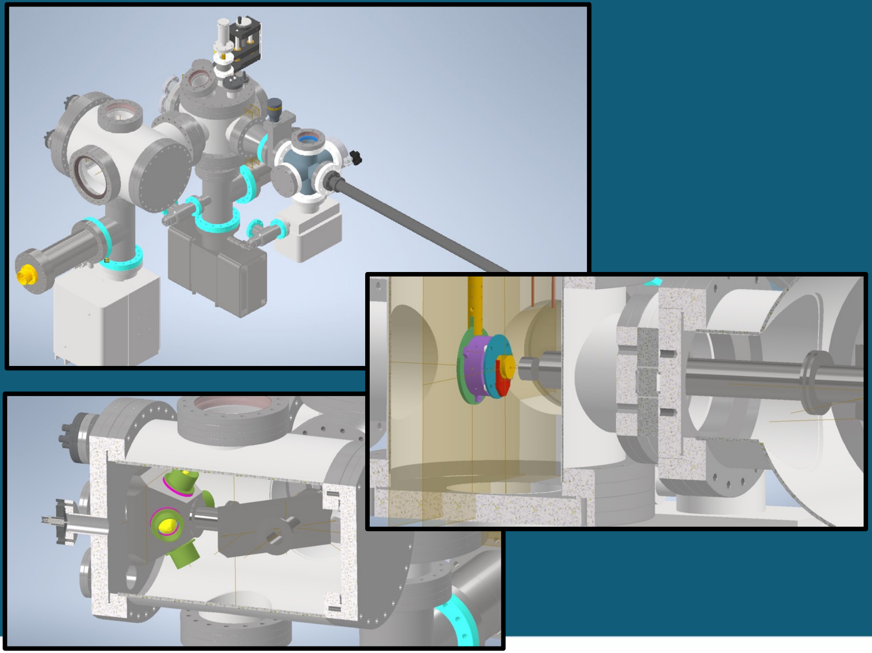

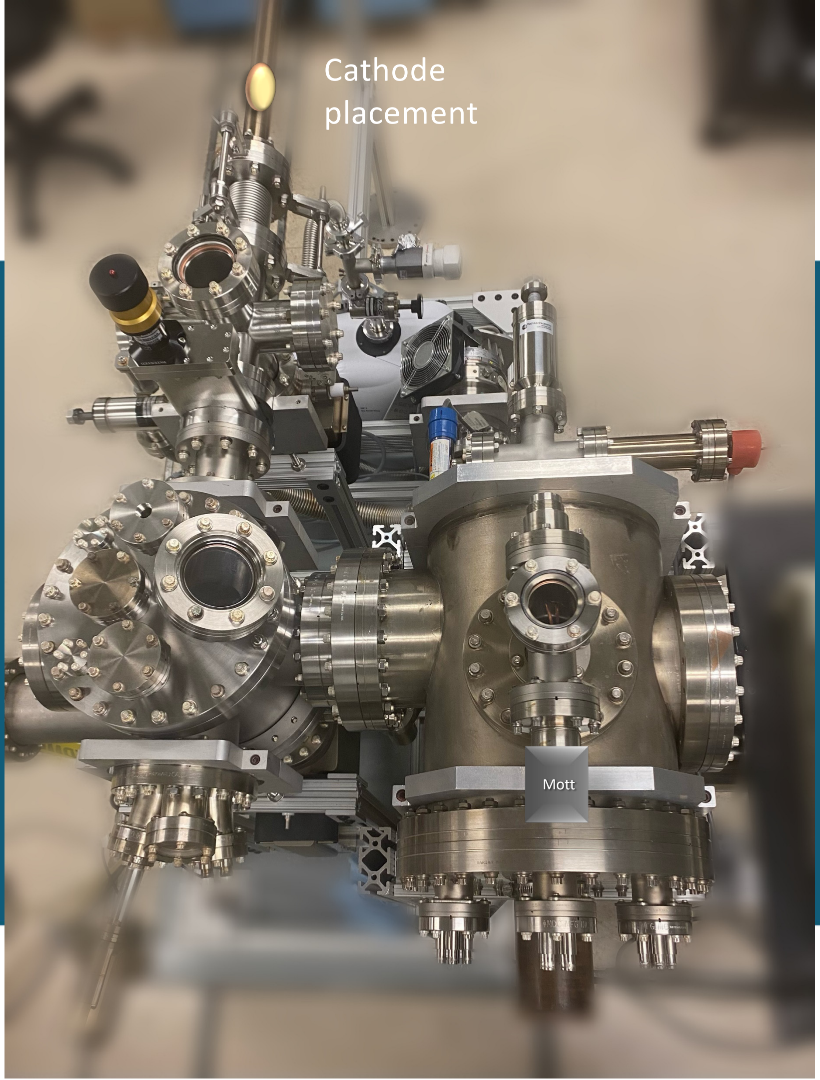

System for electron beam polarization detection

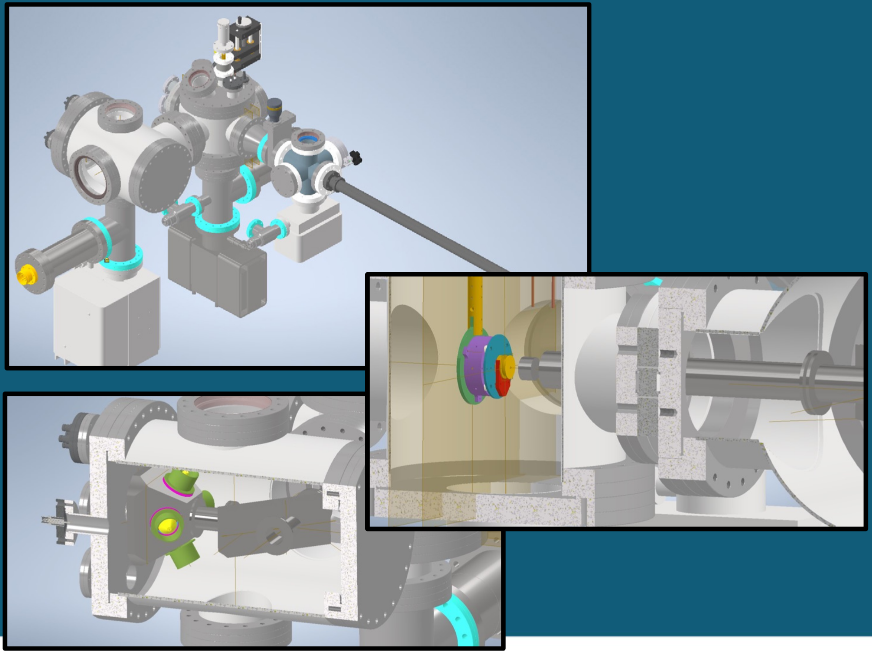

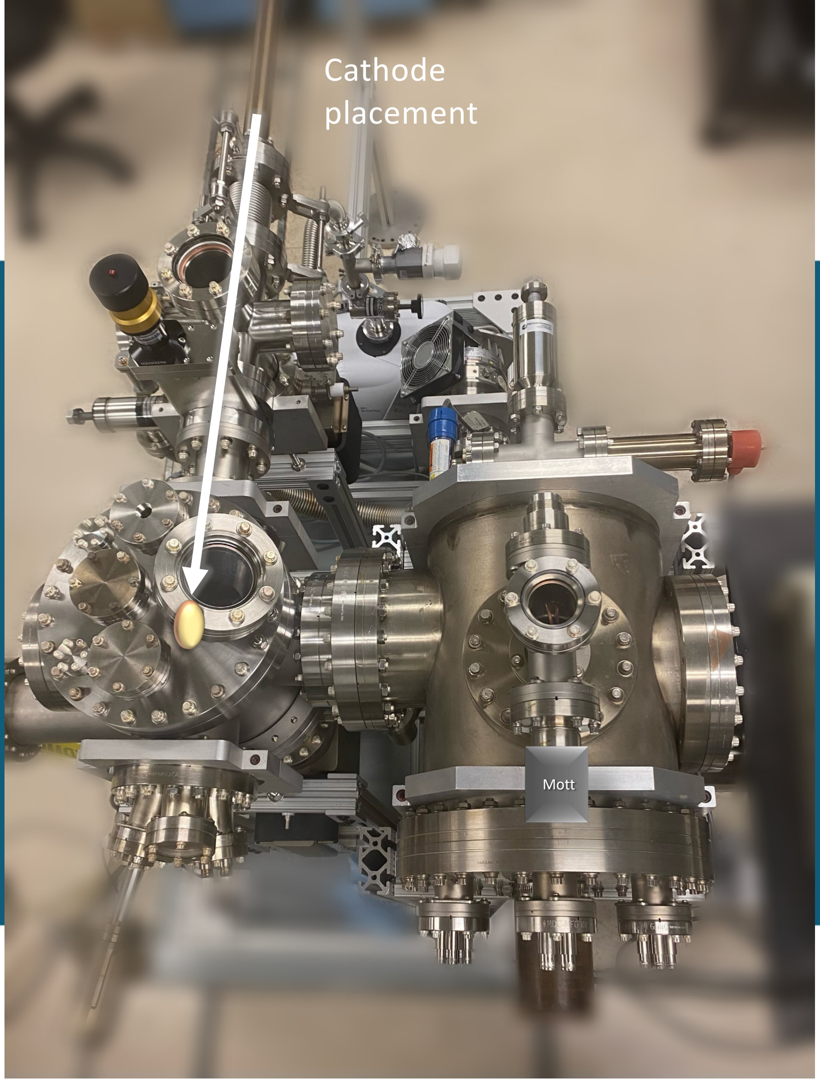

System for electron beam polarization detection

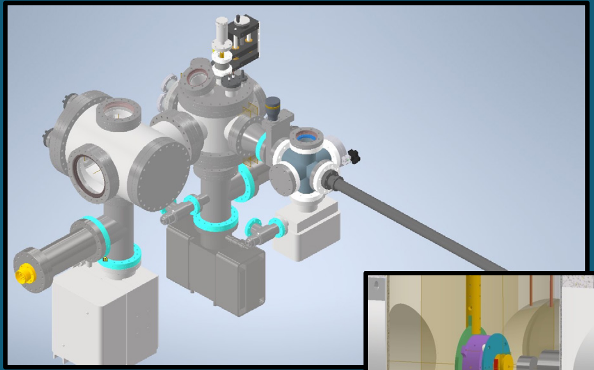

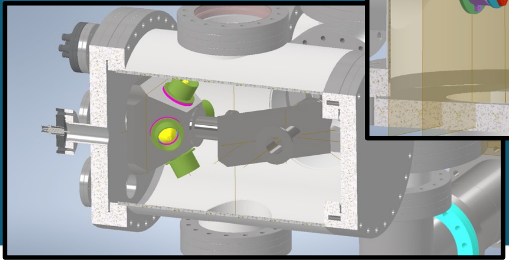

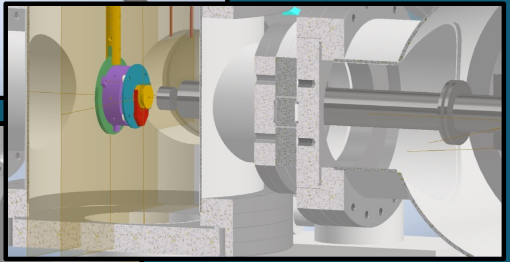

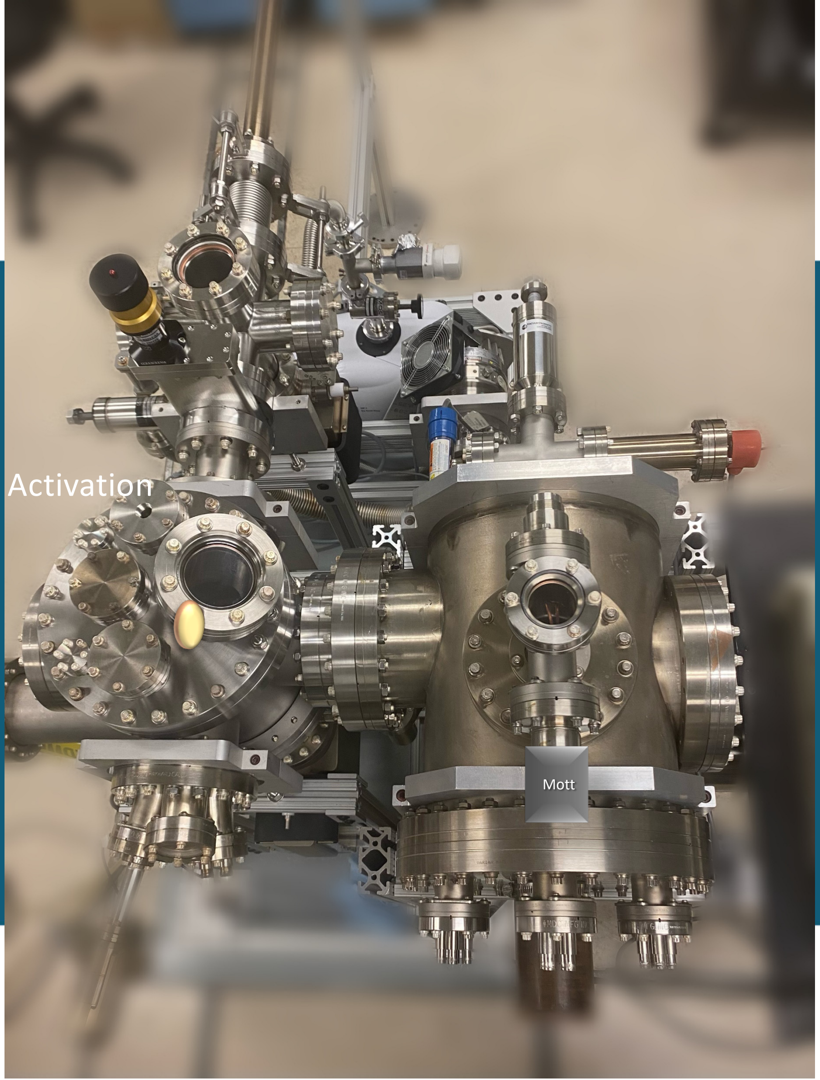

Brookhaven National Laboratory

System for electron beam polarization detection

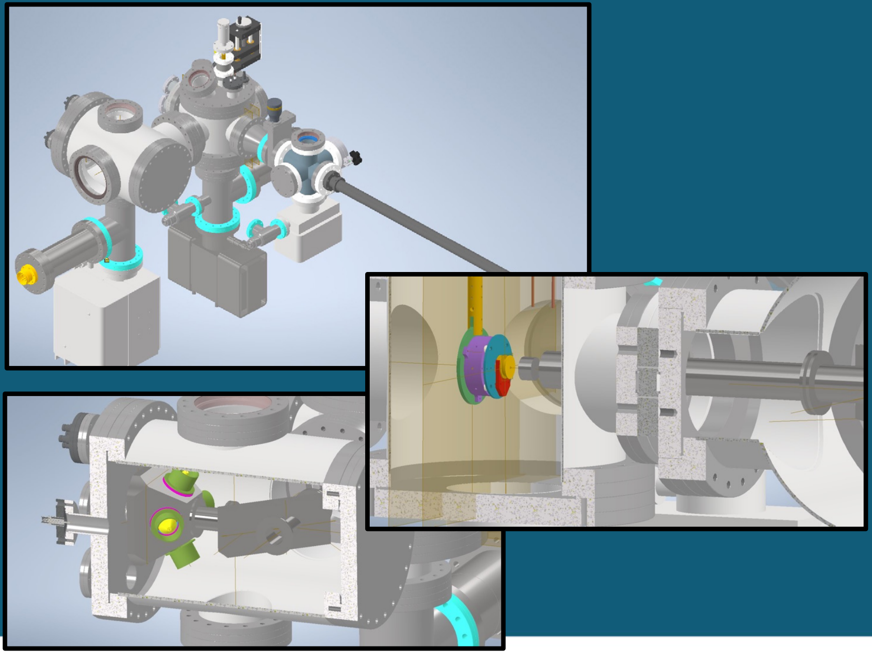

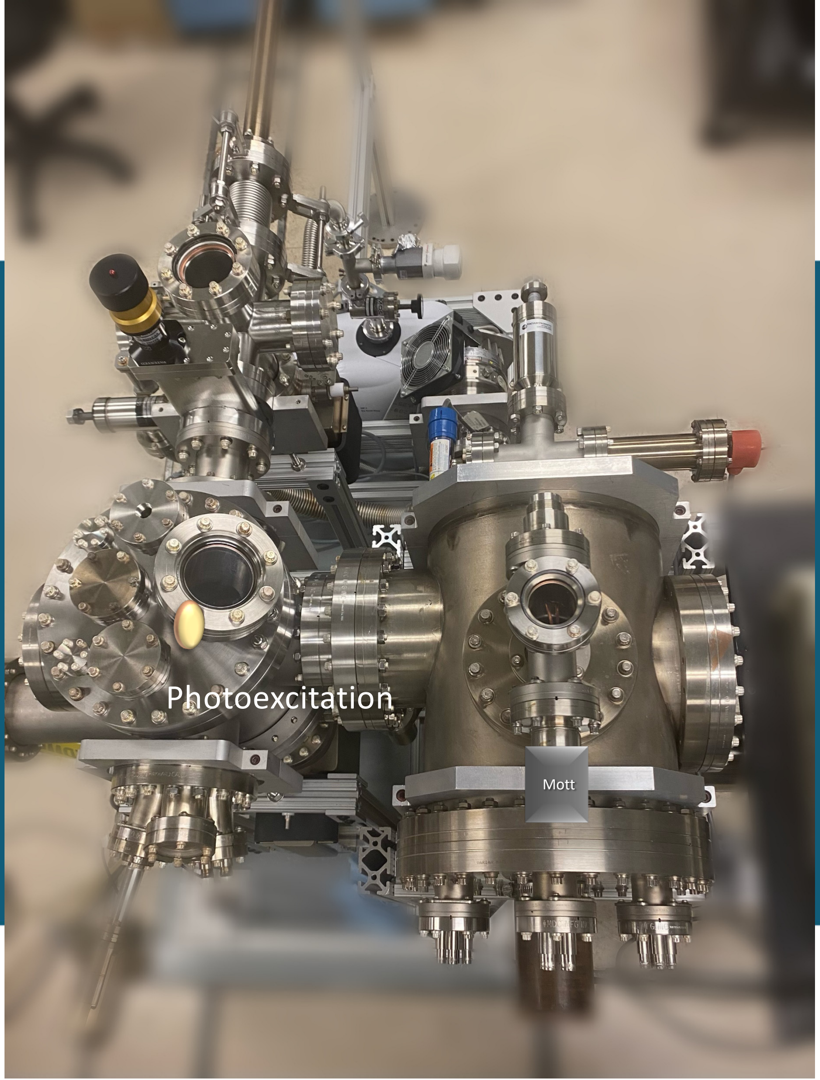

System for electron beam polarization detection

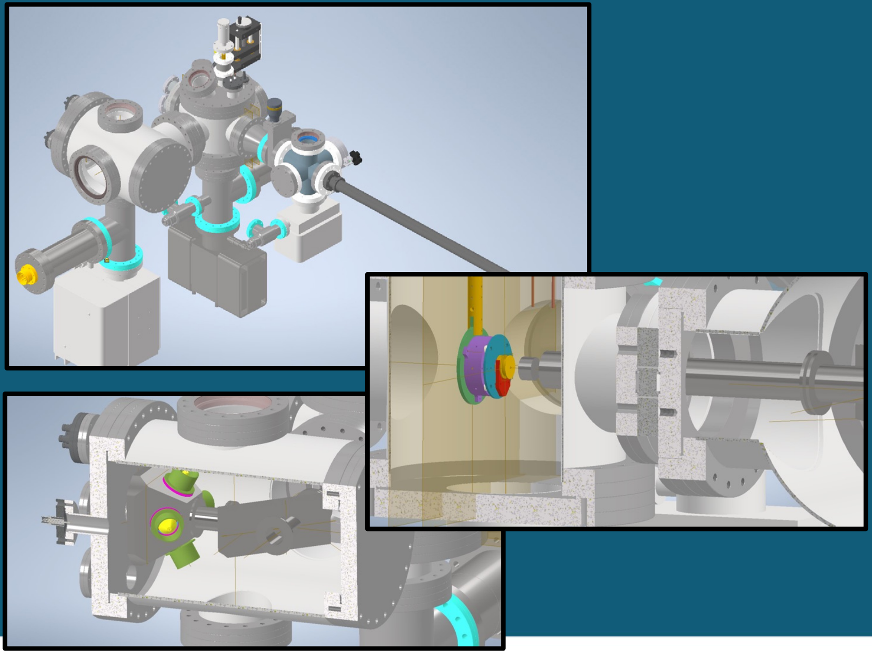

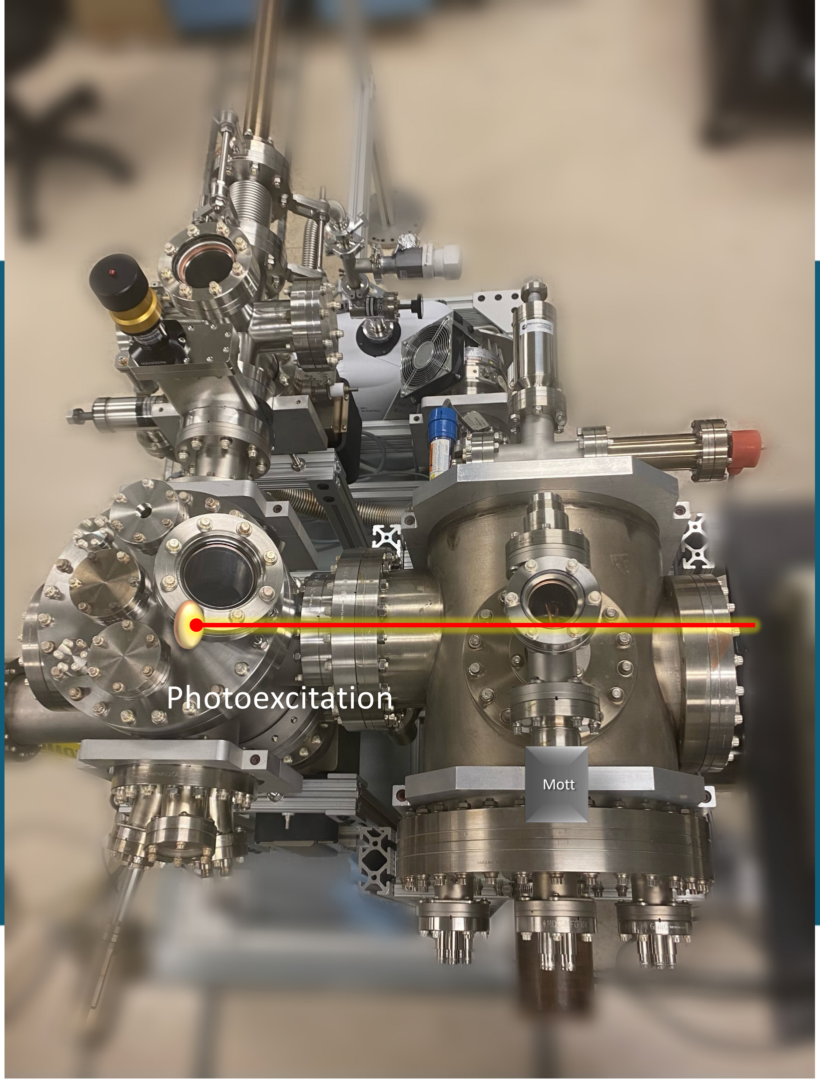

System for electron beam polarization detection

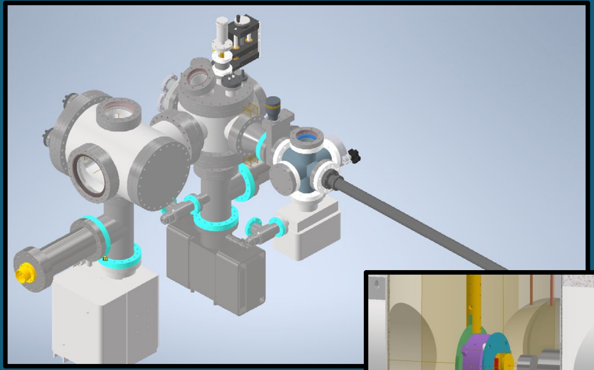

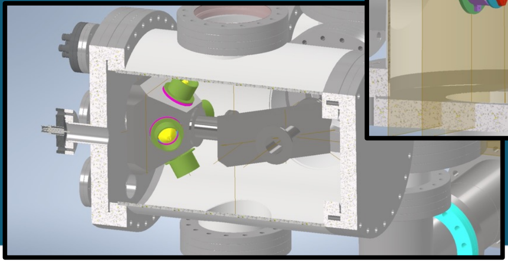

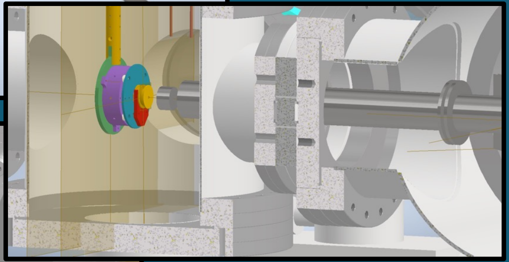

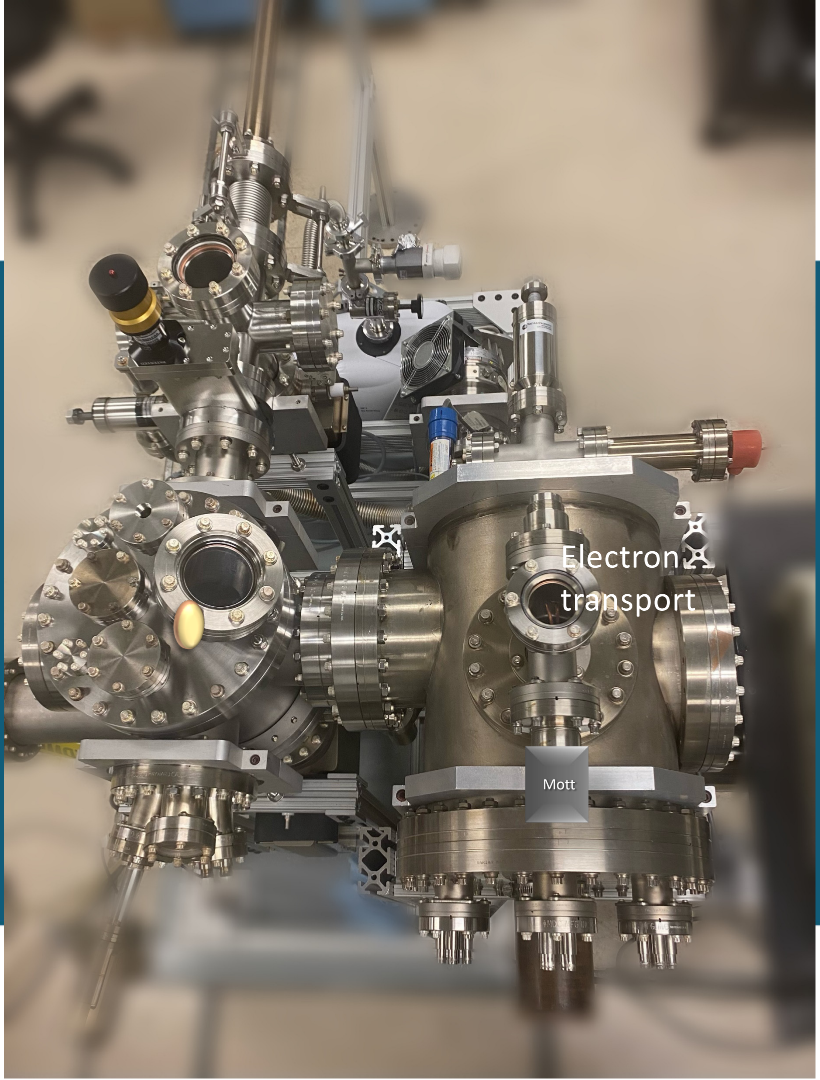

System for electron beam polarization detection

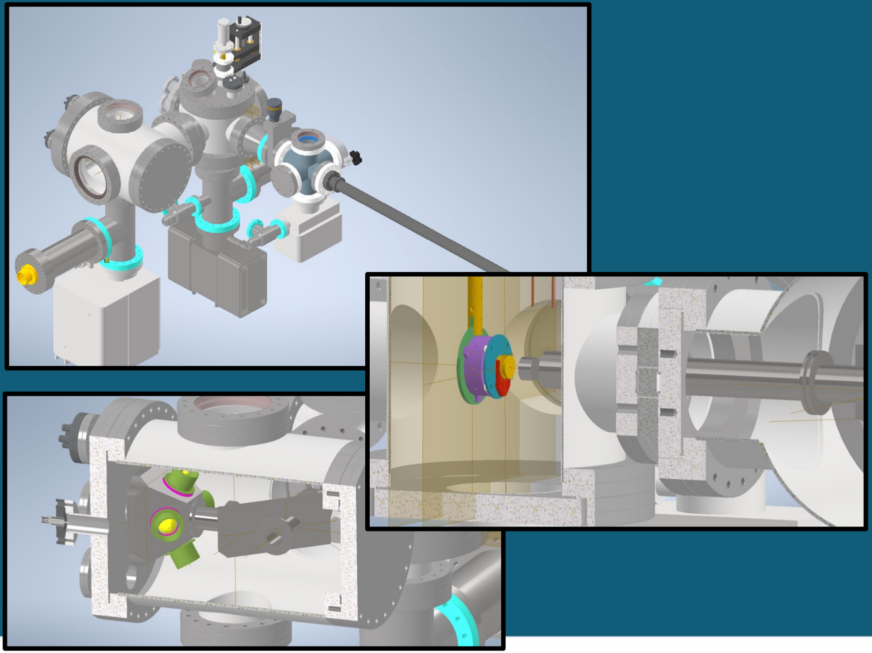

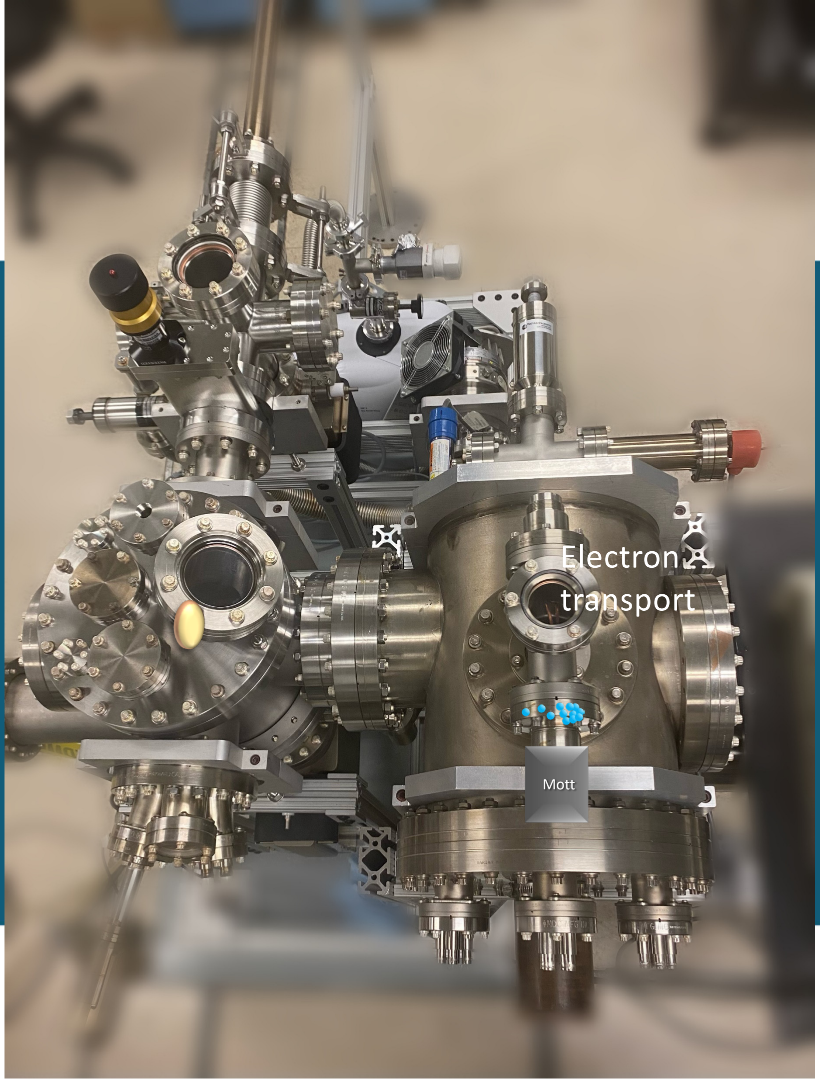

System for electron beam polarization detection

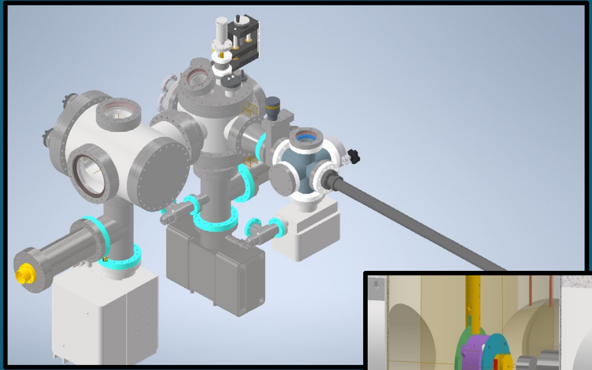

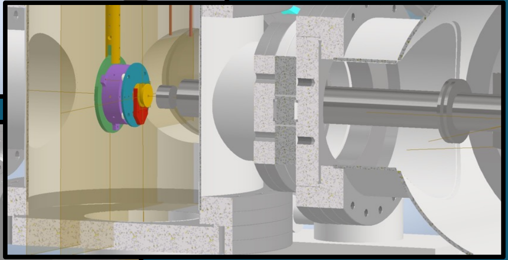

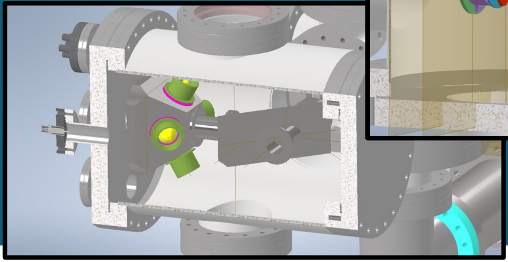

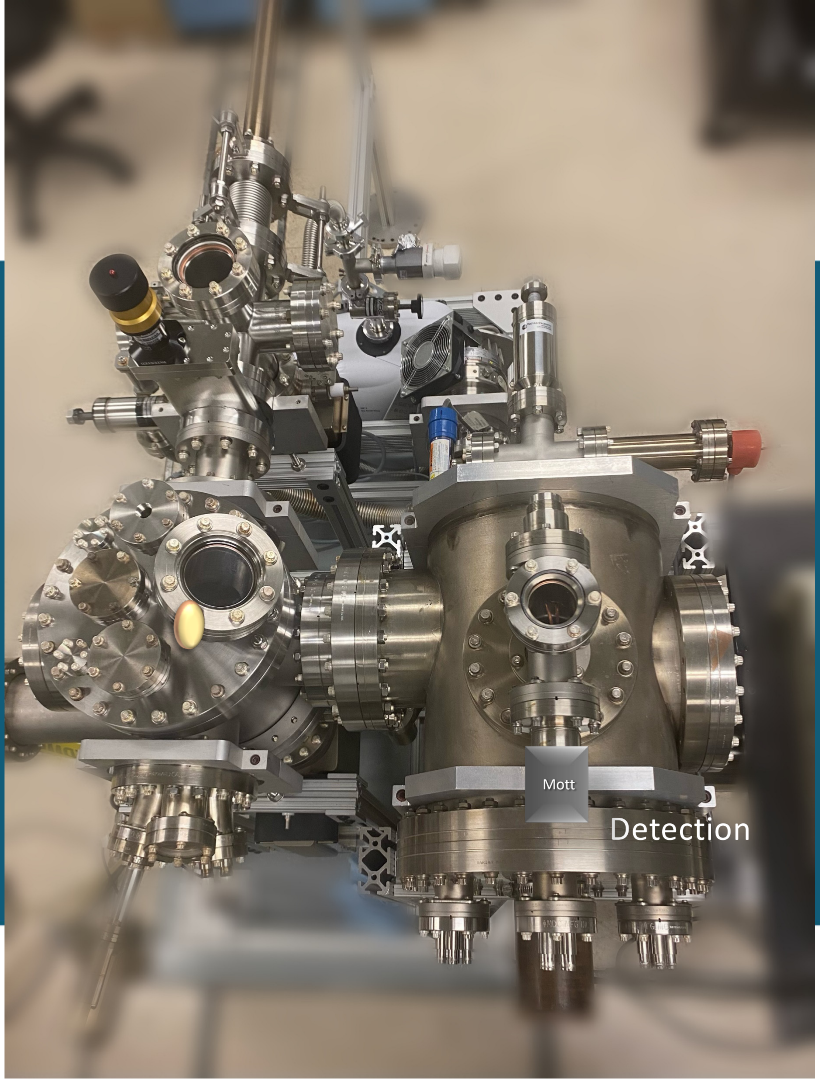

Brookhaven National Laboratory

Other III-Vs current works

Robust Cs-O-Te NEA activation layer

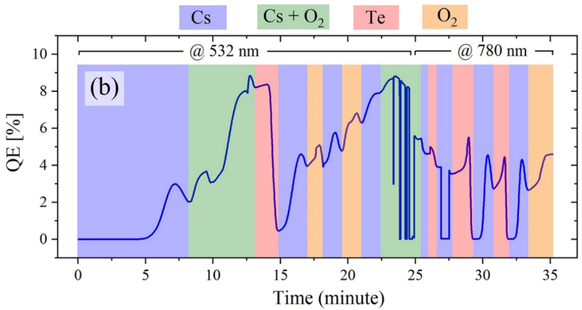

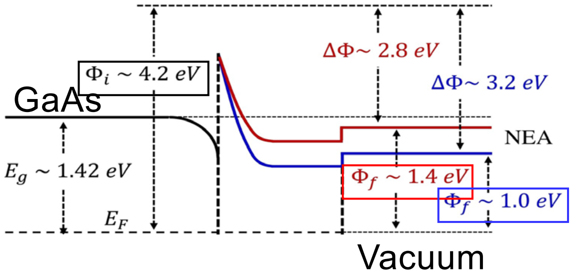

Details to be presented by J. Biswas oral presentation TUYD2

Superlattice with Distributed Bragg Reflector photocathodes

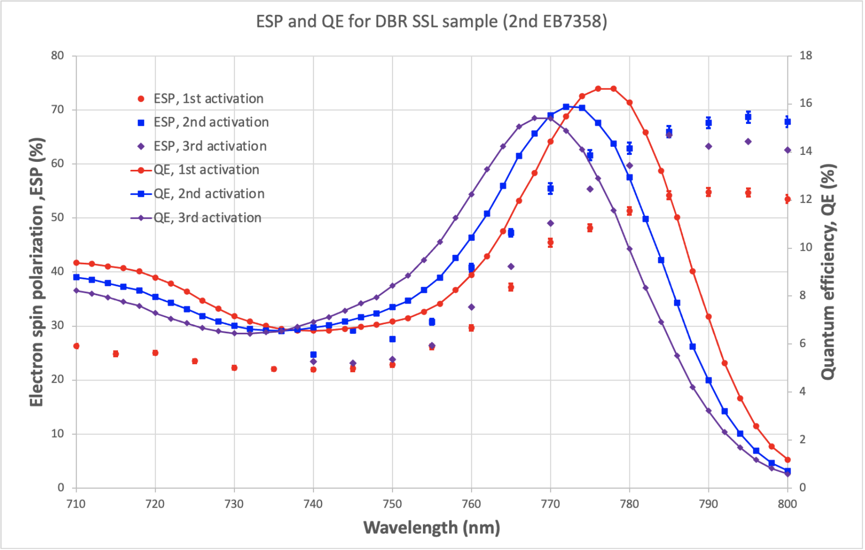

Details can be found in J. Biswas poster presentation

Brookhaven National Laboratory

Acknowledgements

Special thanks to my mentor, Luca Cultrera, for aiding me in understanding the subject and guiding this study, as well as Dr. Palai for his assistance understanding DFT codes and helping with the presentation of the results.

This project was supported in part by the Brookhaven National Laboratory (BNL), Instrumentation Division and the U.S. Department of Energy, Minority Serving Institutions under the Fellowship Program for Research Excellence in Nuclear Physics. The authors also thank the Center for Bright Beams, NSF award PHY-1549132.

Question or comments?